A complex variable meshless local Petrov–Galerkin method for transient heat conduction problems*

Wang Qi-Fang(王启防)[a], Dai Bao-Dong(戴保东)[a]†, and Li Zhen-Feng(栗振锋)[b]

[a] *Department of Engineering Mechanics, Taiyuan University of Science & Technology, Taiyuan* 030024, *China*
[b] *College of Transportation & Logistics, Taiyuan University of Science & Technology, Taiyuan* 030024, *China*

(Received 28 January 2013; revised manuscript received 28 March 2013)

On the basis of the complex variable moving least-square (CVMLS) approximation, a complex variable meshless local Petrov–Galerkin (CVMLPG) method is presented for transient heat conduction problems. The method is developed based on the CVMLS approximation for constructing shape functions at scattered points, and the Heaviside step function is used as a test function in each sub-domain to avoid the need for a domain integral in symmetric weak form. In the construction of the well-performed shape function, the trial function of a two-dimensional (2D) problem is formed with a one-dimensional (1D) basis function, thus improving computational efficiency. The numerical results are compared with the exact solutions of the problems and the finite element method (FEM). This comparison illustrates the accuracy as well as the capability of the CVMLPG method.

Keywords: meshless method, complex variable moving least-square method, complex variable meshless local Petrov–Galerkin method, transient heat conduction problems

PACS: 02.60.Cb, 02.60.Lj, 44.10.+i **DOI:** 10.1088/1674-1056/22/8/080203

1. Introduction

Over the past twenty years, meshless methods have became one of the major interesting focuses in computational mechanics.[1] Today, meshless methods are commonly used in several engineering fields from fluid mechanics to biomechanics. The meshless local Petrov–Galerkin (MLPG) method is one of these meshless schemes. The main advantage of this method over other meshless methods is that this method is a "truly meshless" approach. In other words, no background mesh is required for the interpolation of the solution variables or for the evaluation of the various integrals appearing in the local weak formulation of the problem. The MLPG method has been demonstrated to be quite successful in solving various partial differential equations. The concept of this approach was first introduced by Atluri and Zhu.[2] They solved elastostatic problems in two-dimensional (2D) domains. Recent publications show considerable interest in the development of the MLPG method for a range of problems and physics in analysis of solids such as fracture mechanics,[3] plate bending problems,[4] nonlinear problems,[5] steady-state heat conduction problems,[6] fluid mechanics,[7] etc.

However, in the MLPG method, the lack of Kronecker delta property of the shape functions based on the moving least square (MLS) approximation renders the implementation of essential boundary conditions awkward. Furthermore, the computational cost of the MLS approximation is quite burdensome. Sometimes this method can form an ill-conditioned system of equations. To overcome the shortcomings of the MLS method, Liew *et al.*[8] and Cheng *et al.*[9] proposed a complex variable moving least-square (CVMLS) approximation in which the trial function of a 2D problem is formed with a one-dimensional (1D) basis function. In the CVMLS approximation, the number of unknown coefficients is less than that in the trial function of the MLS approximation. Therefore, the CVMLS approximation has greater computational efficiency.

Based on the CVMLS approximation, many kinds of meshless methods with complex variable have been successfully developed and used to solve a variety of engineering problems. These include the complex variable element-free Galerkin (CVEFG) method,[10–18] the complex variable boundary element-free method for 2D elastodynamics problems,[19] the complex variable meshless local Petrov–Galerkin (CVMLPG) method,[20,21] and the complex variable meshless manifold method (CVMMM).[22,23] On the basis of the reproducing kernel particle method and the complex variable theory, the complex variable reproducing kernel particle method was developed by Chen and Cheng.[24–27]

The main objective of this investigation is to develop the CVMLPG method for transient heat conduction problems. First, the CVMLS approximation and the weak formulations of CVMLPG are briefly introduced; then, the corresponding formulae are obtained. Comparisons are made through some illustrative examples to show the accuracy of the present approach.

*Project supported by the National Natural Science Foundation of China (Grant No. 51078250), the Research Project by Shanxi Scholarship Council of Shanxi Province, China (Grant No. 2013-096), and the Scientific & Technological Innovation Program for Postgraduates of Taiyuan University of Science and Technology, China (Grant No. 20125026).

†Corresponding author. E-mail: Dai_baodong@126.com

© 2013 Chinese Physical Society and IOP Publishing Ltd

2. Complex variable moving least-square approximation

In the CVMLPG method, the variable $\tilde{u}(z)$ of the problem is approximated by the CVMLS approximation scheme.[9]

The CVMLS approximation $u^h(z)$ of $\tilde{u}(z)$ in domain Ω is defined by

$$u^h(z) = u_1^h(z) + \mathrm{i}u_2^h(z) = \sum_{j=1}^{m} p_j(z)\, a_j(z) = \boldsymbol{p}^{\mathrm{T}}(z)\,\boldsymbol{a}(z), \quad (z = x_1 + \mathrm{i}x_2 \in \Omega), \tag{1}$$

where m is the number of terms in the basis function vector, $p_j(z)$ are monomial basis functions, and $a_j(z)$ are the associated coefficients. For example, the basis in 2D is given by

$$\text{Linear basis}: \ \boldsymbol{p}(z) = (1, z)^{\mathrm{T}}, \tag{2}$$

$$\text{Quadratic basis}: \ \boldsymbol{p}(z) = \left(1, z, z^2\right)^{\mathrm{T}}. \tag{3}$$

To approximate $\tilde{u}(z)$ integrally, the local approximation at point z is defined as

$$u^h(z, \bar{z}) = \sum_{j=1}^{m} p_j(\bar{z})\, a_j(z) = \boldsymbol{p}^{\mathrm{T}}(\bar{z})\,\boldsymbol{a}(z), \tag{4}$$

where $\bar{z}$ is the node in the local support domain of point z.

The coefficient vector $\boldsymbol{a}(z)$ is determined by minimizing a weighted discrete L_2 norm, that is by minimizing the weighted discrete norm

$$J = \sum_{I=1}^{n} w(z - z_I)\left[u^h(z, \bar{z}) - \tilde{u}(z_I)\right]^2 = \sum_{I=1}^{n} w(z - z_I)\left[\sum_{j=1}^{m} p_j(\bar{z})\, a_j(z) - \tilde{u}(z_I)\right]^2, \tag{5}$$

where $z_I\,(I = 1, 2, \ldots, n)$ are the nodes in a compact support domain of point z, $w(z - z_I)$ is the test function associated with the node z_I and

$$\tilde{u}(z_I) = u_1(z_I) + \mathrm{i}u_2(z_I). \tag{6}$$

Equation (5) can be described in matrix form as

$$J = (\boldsymbol{P}\boldsymbol{a} - \tilde{\boldsymbol{u}})^{\mathrm{T}}\,\boldsymbol{W}(z)\,(\boldsymbol{P}\boldsymbol{a} - \tilde{\boldsymbol{u}}), \tag{7}$$

where $\tilde{\boldsymbol{u}}$ is the vector of nodal unknowns, and it can be expressed as

$$\tilde{\boldsymbol{u}} = (\tilde{u}(z_1), \tilde{u}(z_2), \ldots, \tilde{u}(z_n))^{\mathrm{T}} = \boldsymbol{Q}\boldsymbol{u}, \tag{8}$$

with

$$\boldsymbol{Q} = \begin{pmatrix} 1 & \mathrm{i} & 0 & 0 & 0 & 0 & \cdots & 0 & 0 \\ 0 & 0 & 1 & \mathrm{i} & 0 & 0 & \cdots & 0 & 0 \\ 0 & 0 & 0 & 0 & 1 & \mathrm{i} & \cdots & 0 & 0 \\ \vdots & \vdots & \vdots & \vdots & \vdots & \vdots & \ddots & \vdots & \vdots \\ 0 & 0 & 0 & 0 & 0 & 0 & \cdots & 1 & \mathrm{i} \end{pmatrix}_{n \times 2n}, \tag{9}$$

$$\boldsymbol{u} = (u_1(z_1), u_2(z_1), u_1(z_2), u_2(z_2), \ldots, u_1(z_n), u_2(z_n))^{\mathrm{T}}, \tag{10}$$

$$\boldsymbol{P} = \begin{pmatrix} p_1(z_1) & p_2(z_1) & \cdots & p_m(z_1) \\ p_1(z_2) & p_2(z_2) & \cdots & p_m(z_2) \\ \vdots & \vdots & \ddots & \vdots \\ p_1(z_n) & p_2(z_n) & \cdots & p_m(z_n) \end{pmatrix}_{n \times m}, \tag{11}$$

$$\boldsymbol{W}(z) = \begin{pmatrix} w(z - z_1) & 0 & \cdots & 0 \\ 0 & w(z - z_2) & \cdots & 0 \\ \vdots & \vdots & \ddots & \vdots \\ 0 & 0 & \cdots & w(z - z_n) \end{pmatrix}_{n \times n}. \tag{12}$$

To obtain $\boldsymbol{a}(z)$, we take the derivative of J with respect to $\boldsymbol{a}(z)$ as follows:

$$\frac{\partial J}{\partial \boldsymbol{a}} = \boldsymbol{A}(z)\,\boldsymbol{a}(z) - \boldsymbol{B}(z)\,\tilde{\boldsymbol{u}} = 0, \tag{13}$$

which results in the equation system

$$\boldsymbol{A}(z)\,\boldsymbol{a}(z) = \boldsymbol{B}(z)\,\tilde{\boldsymbol{u}}, \tag{14}$$

where

$$\boldsymbol{A}(z) = \boldsymbol{P}^{\mathrm{T}}\boldsymbol{W}(z)\,\boldsymbol{P}, \tag{15}$$

$$\boldsymbol{B}(z) = \boldsymbol{P}^{\mathrm{T}}\boldsymbol{W}(z). \tag{16}$$

Then $\boldsymbol{a}(z)$ can be deduced from Eq. (14) as

$$\boldsymbol{a}(z) = \boldsymbol{A}^{-1}(z)\,\boldsymbol{B}(z)\,\tilde{\boldsymbol{u}}. \tag{17}$$

Substituting Eq. (17) into Eq. (4) leads to

$$u^h(z, \bar{z}) = \boldsymbol{\Phi}(z)\,\tilde{\boldsymbol{u}} = \sum_{I=1}^{n} \phi_I(z)\,\tilde{u}(z_I) = u_1^h(z) + \mathrm{i}u_2^h(z). \tag{18}$$

Therefore we have

$$u_1^h(z) = \mathrm{Re}\left[\boldsymbol{\Phi}(z)\,\tilde{\boldsymbol{u}}\right] = \mathrm{Re}\left[\sum_{I=1}^{n} \phi_I(z)\,\tilde{u}(z_I)\right], \tag{19}$$

$$u_2^h(z) = \mathrm{Im}\left[\boldsymbol{\Phi}(z)\,\tilde{\boldsymbol{u}}\right] = \mathrm{Im}\left[\sum_{I=1}^{n} \phi_I(z)\,\tilde{u}(z_I)\right], \tag{20}$$

where $\boldsymbol{\Phi}(z)$ is defined as the shape function vector of the CVMLS method, and

$$\boldsymbol{\Phi}(z) = (\phi_1(z), \phi_2(z), \ldots, \phi_n(z)) = \boldsymbol{p}^{\mathrm{T}}(z)\,\boldsymbol{A}^{-1}(z)\,\boldsymbol{B}(z), \tag{21}$$

with

$$\phi_I(z) = \boldsymbol{p}^{\mathrm{T}}(z)\,\boldsymbol{A}^{-1}(z)\,\boldsymbol{B}_I(z), \tag{22}$$

and the derivate of ϕ_I is

$$\phi_{I,i}(z) = \left(\boldsymbol{p}^{\mathrm{T}}(z)\,\boldsymbol{A}^{-1}(z)\,\boldsymbol{B}_I(z)\right)_{,i} = \boldsymbol{p}_{,i}^{\mathrm{T}}(z)\,\boldsymbol{A}^{-1}(z)\,\boldsymbol{B}_I(z) + \boldsymbol{p}^{\mathrm{T}}(z)\,\boldsymbol{A}^{-1}(z)_{,i}\,\boldsymbol{B}_I(z) + \boldsymbol{p}^{\mathrm{T}}(z)\,\boldsymbol{A}^{-1}(z)\,\boldsymbol{B}_I(z)_{,i}. \tag{23}$$

Compared with the traditional MLS approximation, the CVMLS approximation has the advantages that the trial function of a 2D problem is formed with the 1D basis function, which leads to the fewer nodes used to form the meshless shape function. Consequently the efficiency is improved.

3. CVMLPG method of solving 2D transient heat conduction problems

3.1. Governing equation and its local weak form

Transient heat conduction problems are related to time. The study of this problem can be boiled down to finding the answer to the parabolic partial differential equation. The transient heat conduction equation (2D in this paper) for a stationary medium is given by

$$\rho c\frac{\partial T}{\partial t}-\frac{\partial}{\partial x_1}\left(k_1\frac{\partial T}{\partial x_1}\right)-\frac{\partial}{\partial x_2}\left(k_2\frac{\partial T}{\partial x_2}\right)-Q=0,\ \ (\text{in}\ \ \Omega), \tag{24}$$

where $T=T(x_1,x_2,t)$ represents the temperature field, t is time ($t\geq 0$), ρ and c are the density of material and specific heat capacity, respectively, k_1 and k_2 denote the thermal conductivities along the x_1 and x_2 directions, respectively, Q is the heat generation per unit volume, and Ω is the 2D domain bounded by Γ, with $\Gamma=\Gamma_1\cup\Gamma_2\cup\Gamma_3$.

The initial and boundary conditions for this type of problem are

$$T(x_1,x_2,0)=T_0,\ \ (\text{when}\ \ t=0), \tag{25}$$

$$T-\bar{T}=0,\ \ (\text{on}\ \ \Gamma_1), \tag{26}$$

$$k_1\frac{\partial T}{\partial x_1}n_1+k_2\frac{\partial T}{\partial x_2}n_2-\bar{q}=0,\ \ (\text{on}\ \Gamma_2), \tag{27}$$

$$k_1\frac{\partial T}{\partial x_1}n_1+k_2\frac{\partial T}{\partial x_2}n_2-h(T_a-T)=0,\ \ (\text{on}\ \ \Gamma_3), \tag{28}$$

where Γ_1, Γ_2, and Γ_3 denote the Dirichlet, Neumann, and Robin boundary conditions, respectively; $\bar{T}$, $\bar{q}$, and h are the prescribed initial temperature, the prescribed density of the heat flux, and the convection heat transfer coefficient on boundary Γ_1, Γ_2, and Γ_3, respectively; n_1 and n_2 are direction cosines pointing outward to the boundary Γ_3 in x_1 and x_2 directions, respectively; T_a is surrounding fluid temperature.

Local weighted residual method is employed in the sub-domain Ω_S to create the system of equations. We can obtain

$$\int_{\Omega_S}v_I\left[\rho c\frac{\partial T}{\partial t}-\frac{\partial}{\partial x_1}\left(k_1\frac{\partial T}{\partial x_1}\right)-\frac{\partial}{\partial x_2}\left(k_2\frac{\partial T}{\partial x_2}\right)-Q\right]\mathrm{d}\Omega=0, \tag{29}$$

where Ω_S bounded by Γ_S is the sub-domain associated with node z_I, and v_I is the test function in Ω_S.

To reduce this high-order differentiability requirement on T, we can integrate Eq. (29) by parts. Using Gauss's theorem, we can obtain the following local weak formulation:

$$\int_{\Omega_S}\left(v_I\rho c\frac{\partial T}{\partial t}+k_1\frac{\partial T}{\partial x_1}\frac{\partial v_I}{\partial x_1}+k_2\frac{\partial T}{\partial x_2}\frac{\partial v_I}{\partial x_2}-v_IQ\right)\mathrm{d}\Omega=\int_{\Gamma_S}\left(v_Ik_1\frac{\partial T}{\partial x_1}n_1+v_Ik_2\frac{\partial T}{\partial x_2}n_2\right)\mathrm{d}\Gamma. \tag{30}$$

Substituting Eqs. (27) and (28) into Eq. (30) leads to

$$\int_{\Omega_S}\left(v_I\rho c\frac{\partial T}{\partial t}+k_1\frac{\partial T}{\partial x_1}\frac{\partial v_I}{\partial x_1}+k_2\frac{\partial T}{\partial x_2}\frac{\partial v_I}{\partial x_2}-v_IQ\right)\mathrm{d}\Omega=\int_{\Gamma_1}\left(v_Ik_1\frac{\partial T}{\partial x_1}n_1+v_Ik_2\frac{\partial T}{\partial x_2}n_2\right)\mathrm{d}\Gamma+\int_{\Gamma_2}v_I\bar{q}\,\mathrm{d}\Gamma+\int_{\Gamma_3}v_Ih(T_a-T)\,\mathrm{d}\Gamma. \tag{31}$$

From Ref. [28], equation (31) can be simplified further into the following equation:

$$\int_{\Omega_S}\left(v_I\rho c\frac{\partial T}{\partial t}+k_1\frac{\partial T}{\partial x_1}\frac{\partial v_I}{\partial x_1}+k_2\frac{\partial T}{\partial x_2}\frac{\partial v_I}{\partial x_2}-v_IQ\right)\mathrm{d}\Omega=\int_{\Gamma_2}v_I\bar{q}\,\mathrm{d}\Gamma+\int_{\Gamma_3}v_Ih(T_a-T)\,\mathrm{d}\Gamma. \tag{32}$$

In order to simplify Eq. (32), the Heaviside step function is chosen as the test function v_I in each sub-domain Ω_S,

$$v_I=\begin{cases}1, & z\in\Omega_S,\\ 0, & z\notin\Omega_S.\end{cases} \tag{33}$$

Then equation (32) can be transformed into the following equation:

$$\int_{\Omega_S}\rho c\frac{\partial T}{\partial t}\mathrm{d}\Omega+\int_{\Gamma_3}hT\,\mathrm{d}\Gamma=\int_{\Omega_S}Q\mathrm{d}\Omega+\int_{\Gamma_2}\bar{q}\mathrm{d}\Gamma+\int_{\Gamma_3}hT_a\mathrm{d}\Gamma. \tag{34}$$

3.2. Discretization of the local weak form

From Eq. (18), temperature $T(z,t)$ at any point z in the domain Ω is given by

$$T(z,t)=\mathrm{Re}[\boldsymbol{\Phi}(z)\boldsymbol{T}]=\sum_{I=1}^{n}\mathrm{Re}[\phi_I(z)T_I]=\sum_{I=1}^{n}\tilde{\phi}_IT_I=\tilde{\boldsymbol{\Phi}}(z)\boldsymbol{T}, \tag{35}$$

$$T_I=T(z_I,t), \tag{36}$$

where

$$\boldsymbol{T}=(T_1,T_2,\ldots,T_n)^{\mathrm{T}}, \tag{37}$$

$$\tilde{\boldsymbol{\Phi}}(z)=\left(\tilde{\phi}_1(z),\tilde{\phi}_2(z),\cdots,\tilde{\phi}_n(z)\right), \tag{38}$$

$$\tilde{\phi}_I(z)=\mathrm{Re}[\phi_I(z)]. \tag{39}$$

Let

$$\frac{\partial T(z,t)}{\partial t}=\frac{\partial}{\partial t}\sum_{I=1}^{n}\mathrm{Re}[\phi_I(z)T_I]=\sum_{I=1}^{n}\mathrm{Re}\left[\phi_I(z)\frac{\partial T_I}{\partial t}\right]=\tilde{\boldsymbol{\Phi}}(z)\dot{\boldsymbol{T}}, \tag{40}$$

where

$$\dot{\boldsymbol{T}}=\left(\frac{\partial T_1}{\partial t},\frac{\partial T_2}{\partial t},\ldots,\frac{\partial T_n}{\partial t}\right)^{\mathrm{T}}. \tag{41}$$

For the discretization of the local weak form, we substitute Eqs. (35) and (40) into the local weak form Eq. (34) and then the sum of all nodes gives the following linear system of ordinary differential equations:

$$\boldsymbol{C}\dot{\boldsymbol{T}} + \boldsymbol{K}\boldsymbol{T} = \boldsymbol{F}, \tag{42}$$

where

$$C_{IJ} = \int_{\Omega_S} \rho c \tilde{\phi}_J \, \mathrm{d}\Omega, \tag{43}$$

$$K_{IJ} = \int_{\Gamma_3} h \tilde{\phi}_J \, \mathrm{d}\Gamma, \tag{44}$$

$$F_I = \int_{\Omega_S} Q \, \mathrm{d}\Omega + \int_{\Gamma_2} \bar{q} \, \mathrm{d}\Gamma + \int_{\Gamma_3} h T_a \, \mathrm{d}\Gamma. \tag{45}$$

Up to now the partial differential equation (24) has been discretized into the ordinary differential equation (42), in which the time is the only independent variable.

3.3. Time difference scheme

Because equation (42) is a linear system of ordinary differential equations, in which the time is the only independent variable. So the traditional two-point difference method is used for time discretization. The relation between $\boldsymbol{T}_{t-\Delta t}$ and $\boldsymbol{T}_t$ can be written as

$$\theta \frac{\mathrm{d}\boldsymbol{T}_t}{\mathrm{d}t} + (1-\theta)\frac{\mathrm{d}\boldsymbol{T}_{t-\Delta t}}{\mathrm{d}t} = \frac{1}{\Delta t}(\boldsymbol{T}_t - \boldsymbol{T}_{t-\Delta t}), \tag{46}$$

where $0 \le \theta \le 1$. The integral is proceed in Crank–Nicolson (CN) format when $\theta = 1/2$. Substituting Eq. (46) ($\theta = 1/2$) into Eq. (42), the following equation is obtained:

$$\begin{aligned}(\boldsymbol{K}/2 + \boldsymbol{C}/\Delta t)\boldsymbol{T}_t = (\boldsymbol{F}_t + \boldsymbol{F}_{t-\Delta t})/2 \\ + (\boldsymbol{C}/\Delta t - \boldsymbol{K}/2)\boldsymbol{T}_{t-\Delta t}.\end{aligned} \tag{47}$$

Equation (47) is the basic equation which solves transient temperatures in CN format.

4. Numerical examples

To verify the validity and efficiency of the CVMLPG method, some numerical examples are given in this section. In our computation, a regular arrangement of nodes is used to numerically calculate the system equation. The linear basis function is used in the present method.

For the purpose of error estimation and convergence studies, the root-mean-square (RMS) error $E_2(t_n)$ and the relative error are usually defined as

$$E_2(t_n) = \frac{1}{N}\sqrt{\sum_{i=1}^{N}(u_i^{\mathrm{num}} - u_i^{\mathrm{exact}})^2} \tag{48}$$

and

$$r = \frac{1}{N}\sqrt{\sum_{i=1}^{N}\left|\frac{u_i^{\mathrm{num}} - u_i^{\mathrm{exact}}}{u_i^{\mathrm{exact}}}\right|^2}, \tag{49}$$

where N is the number of sample points; u_i^{num} and u_i^{exact} refer to the values at the i-th sample point, obtained by the CVMLPG method and analytical solution, respectively.

The first example considered is the problem of 2D transient heat conduction in square domain and the length of the side is π mm. The surrounding temperature is given by $T = 0\ ^\circ\mathrm{C}$, without inner heat source. The parameters of the material are the thermal conductivities $k_1 = k_2 = 10^3\ \mathrm{W/m\cdot{}^\circ C}$, the specific heat capacity $c = 10^3\ \mathrm{J/kg\cdot{}^\circ C}$, and the density $\rho = 10^3\ \mathrm{kg/m^3}$.

The initial temperature is

$$T(x_1, x_2, 0) = 10 \sin x_1 \sin x_2.$$

The analytical solution of this problem is

$$T(x_1, x_2, t) = 10\,\mathrm{e}^{-2t} \sin x_1 \sin x_2.$$

As shown in Fig. 1, 11×11 nodes are uniformly distributed in the domain Ω. Time step is $\Delta t = 0.02$ s in the computing process. The analytical solutions and numerical solutions along $x_2 = \pi/2$ mm when $t = 1$ s, $t = 2$ s, $t = 3$ s are shown in Fig. 2. The distributions of the temperatures at point $A(\pi/4, \pi/4)$ and point $B(\pi/2, \pi/2)$ are shown in Fig. 3, from which we can see that the results obtained from the CVMLPG method are in excellent agreement with the analytical solutions.

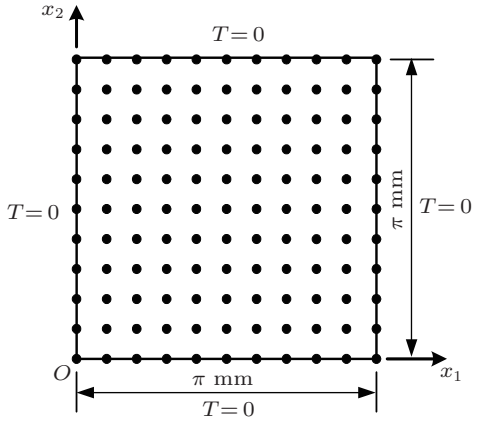


Fig. 1. Node distribution for the first example.

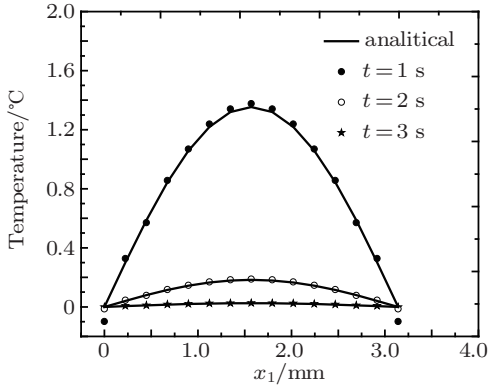


Fig. 2. Temperature distribution at $x_2 = \pi/2$ mm.

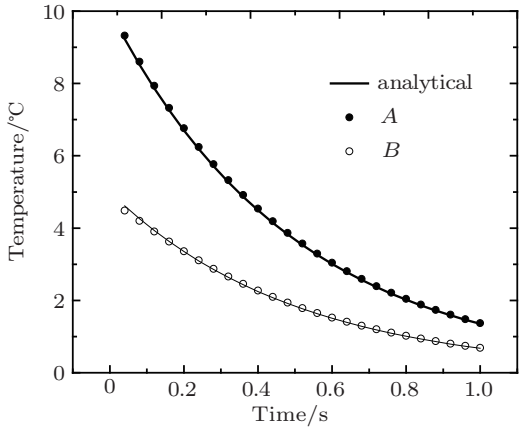


Fig. 3. Variations of temperature at two points $A(\pi/4,\pi/4)$ and $B(\pi/2,\pi/2)$.

In addition, the values of root-mean-square error $E_2(t_n)$ at different times are given in Fig. 4 and the time step is $\Delta t = 0.02$ s, which shows that the numerical solution converges as the time increases. Next, to further verify the accuracy of the CVMLPG method, the relationship between the relative error and the time step is shown in Fig. 5, which demonstrates that the relative error decreases with time step decreasing. From the above figures, we conclude that the method is feasible and valid.

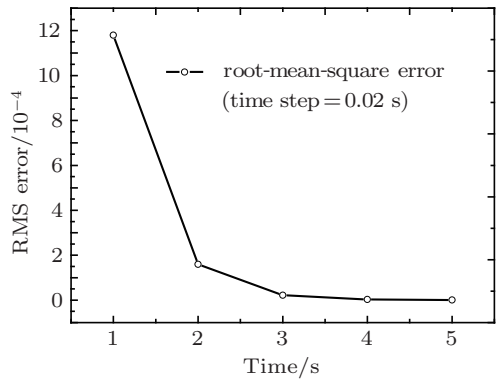


Fig. 4. Variation of root-mean-square error with time.

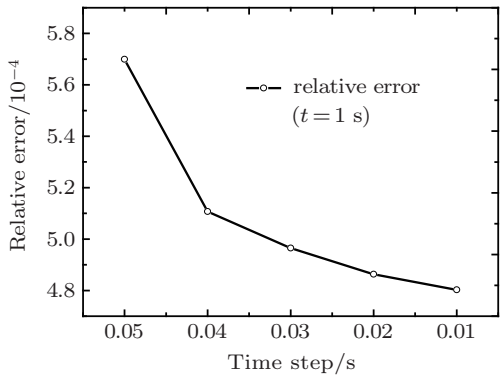


Fig. 5. Relation between time step Δt and relative error when $t = 1$ s.

The second example considered is the transient temperature in the rectangular domain Ω. Its governing equation is written as

$$\frac{\partial T}{\partial t} - \frac{\partial^2 T}{\partial x_1^2} - \frac{\partial^2 T}{\partial x_2^2} = 0,$$
$$x_1 \in [0,\ 1\ \text{mm}], \quad x_2 \in [0,\ 1\ \text{mm}].$$

The boundary conditions are

$$T(0,x_2,t) = \mathrm{e}^{-2t}\sin x_2, \quad T(1,x_2,t) = \mathrm{e}^{-2t}\sin(1+x_2),$$
$$T(x_1,0,t) = \mathrm{e}^{-2t}\sin x_1, \quad T(x_1,1,t) = \mathrm{e}^{-2t}\sin(1+x_1).$$

The initial condition is

$$T(x_1,x_2) = \sin(x_1+x_2) \quad (t=0).$$

As shown in Fig. 6, a regular distribution of 13×13 nodes is used in the domain Ω. The time step is chosen to be $\Delta t = 0.01$ s. The analytical and numerical solutions along $x_1 = 1$ mm and $x_1 = 0$ when $t = 0.1$ s are plotted in Fig. 7 and Fig. 8, respectively. Again, the numerical results show excellent agreement with the analytical solutions.

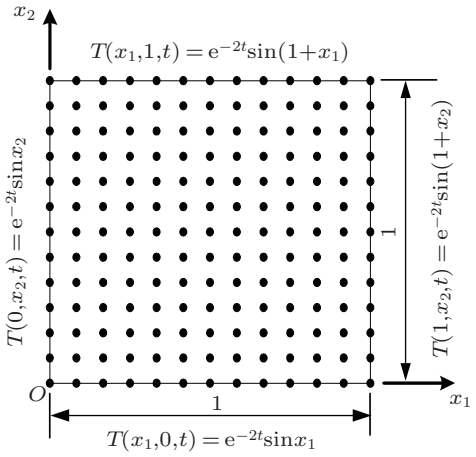


Fig. 6. Node distribution for the second example.

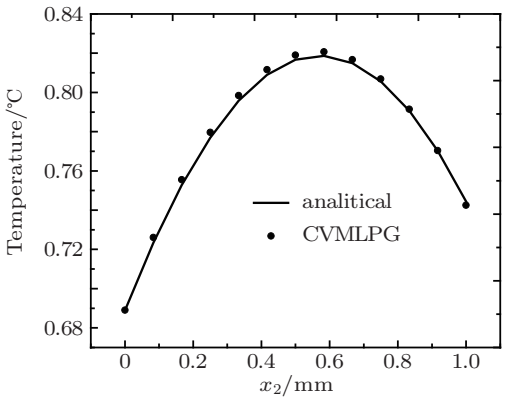


Fig. 7. Temperature distribution at $x_1 = 1$ mm.

The third example presented here is the transient heat conduction problem in square domain and the lengths of the domain sides each are 100 mm. Temperature on the right surface is $T = 0$ °C. The top and bottom surface are insulated. The other parameters of the material are as follows: the thermal conductivities $k_1 = k_2 = 1.6 \times 10^4$ W/m·°C, the specific heat capacity $c = 10^3$ J/kg·°C, and the density $\rho = 10^3$ kg/m^3. Assume that the initial temperature is zero and the temperature on the left surface is $T(0, x_2, t) = T_H[1 - \cos(\omega t)]$, where $T_H = 10$ °C, $\omega = \pi/100$ rad/s.

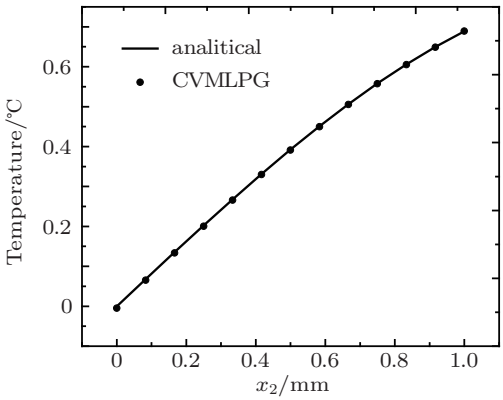


Fig. 8. Temperature distribution at $x_1 = 0$ mm.

As figure 9 shows, 11×11 nodes are distributed in the square domain. The time step is $\Delta t = 0.125$ s. Because of the absence of an analytical solution, the comparison between the CVMLPG and FEM solution is given in Fig. 10, which shows the time history of temperature at point $A(10, 50)$. It is evident that the results from the CVMLPG method accord well with the FEM's results.

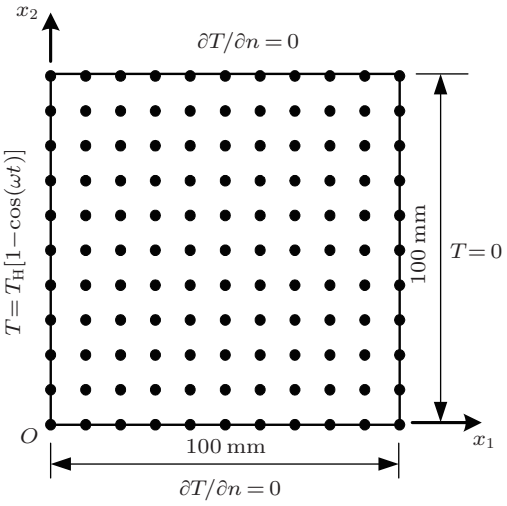


Fig. 9. Node distribution for the third example.

The last example considered is the transient heat conduction problem in an irregular domain and the sizes of each side of this domain are shown in Fig. 11. The temperature on the left surface is $T = 100[1 - \cos(\pi t)]$, the initial temperatures on the other sides are all zero. Other parameters are thermal conductivities $k_1 = k_2 = 1.6 \times 10^4$ W/m·°C, specific heat capacity $c = 10^3$ J/kg·°C, and density $\rho = 10^3$ kg/m^3.

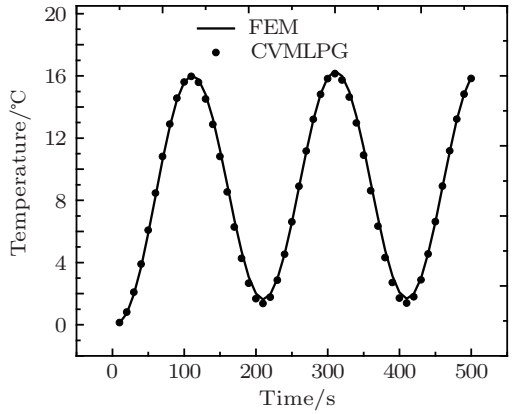


Fig. 10. Comparison of the CVMLPG results with FEM results.

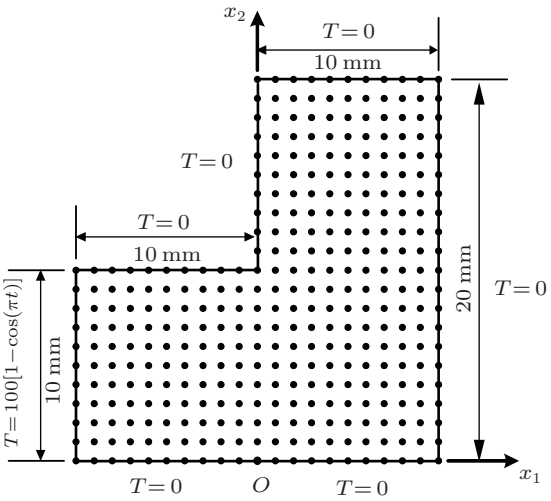


Fig. 11. Node distribution for the last example.

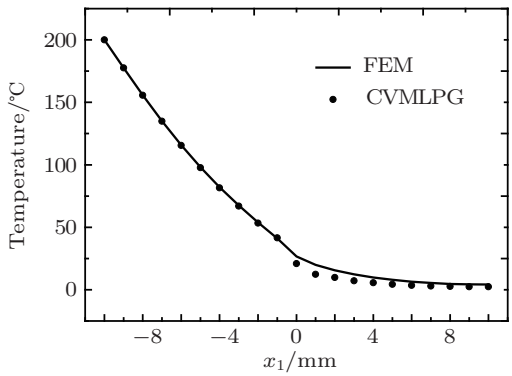


Fig. 12. Comparison of the CVMLPG results with FEM results.

The time step is chosen to be $\Delta t = 0.01$ s. The comparison of the results of CVMLPG with FEM by ABAQUS at

$x_2 = 10$ mm when $t = 1$ s is shown in Fig. 12. Just as we can see that the CVMLPG numerical results match well with the numerical results from ABAQUS, this example confirms that the developed method in this paper can be successfully used to solve the transient heat conduction problem with an irregular domain.

5. Conclusions

A new local meshless methodology, called the CVMLPG method, has been developed for problems of transient heat conduction. In the present method, the CVMLS approximation is employed to construct the shape functions. The trial function of a 2D problem is formed with a 1D basis function. The number of unknown coefficients in the trial function of the CVMLS approximation is less than that in the trial function of the MLS. This substantially reduces the computational efforts needed for constructing the stiffness matrix. Hence, the present approach is computationally efficient compared with the conventional MLPG method. The numerical results demonstrate that the CVMLPG method presented in this paper is both feasible and effective.

References

[1] Zhang X, Liu Y and Ma S 2009 *Adv. Mech.* **39** 1
[2] Atluri S N and Zhu T L 1998 *Comput. Mech.* **22** 117
[3] Ching H K and Batra R C 2001 *Comput. Model. Eng. Sci.* **2** 273
[4] Long S Y and Atluri S N 2002 *Comput. Model. Eng. Sci.* **3** 53
[5] Han Z D, Rajendran A M and Atluri S N 2005 *Comput. Model. Eng. Sci.* **10** 1
[6] Wu X H and Tao W Q 2008 *Int. J. Heat Mass Transfer* **51** 3103
[7] Lin H and Atluri S N 2001 *Comput. Model. Eng. Sci.* **2** 117
[8] Liew K M, Feng C, Cheng Y and Kitipornchai S 2007 *Int. J. Numer. Meth. Eng.* **70** 46
[9] Cheng Y M, Peng M J and Li J H 2005 *Chin. J. Theor. Appl. Mech.* **37** 1
[10] Peng M J, Liu P and Cheng Y M 2009 *Int. J. Appl. Mech.* **1** 367
[11] Bai F N, Li D M, Wang J F and Cheng Y M 2012 *Chin. Phys. B* **21** 020204
[12] Peng M J, Li D M and Cheng Y M 2011 *Engin. Struct.* **33** 127
[13] Li D M, Bai F N, Cheng Y M and Liew K M 2012 *Comp. Meth. Appl. Mech. Eng.* **233–236** 1
[14] Cheng Y M, Li R X and Peng M J 2012 *Chin. Phys. B* **21** 090205
[15] Wang J F and Cheng Y M 2012 *Chin. Phys. B* **21** 120206
[16] Cheng Y M, Wang J F and Li R X 2012 *Int. J. Appl. Mech.* **4** 1250042
[17] Cheng Y M, Wang J F and Bai F N 2012 *Chin. Phys. B* **21** 090203
[18] Wang J F and Cheng Y M 2013 *Chin. Phys. B* **22** 030208
[19] Liew K M and Cheng Y M 2009 *Comp. Meth. Appl. Mech. Eng.* **198** 3925
[20] Yang X L, Dai B D and Li Z F 2012 *Acta Phys. Sin.* **61** 050204 (in Chinese)
[21] Yang X L, Dai B D and Zhang W W 2012 *Chin. Phys. B* **21** 100208
[22] Gao H F and Cheng Y M 2009 *Chin. J. Theor. Appl. Mech.* **41** 480
[23] Gao H F and Cheng Y M 2010 *Int. J. Comput. Meth.* **7** 55
[24] Chen L and Cheng Y M 2008 *Acta Phys. Sin.* **57** 1 (in Chinese)
[25] Chen L and Cheng Y M 2008 *Acta Phys. Sin.* **57** 6047 (in Chinese)
[26] Chen L and Cheng Y M 2010 *Chin. Phys. B* **19** 090204
[27] Chen L and Cheng Y M 2010 *Sci. China G: Phys. Mech. Astron.* **40** 242
[28] Li Q H, Chen S S and Kou G X 2011 *J. Comput. Phys.* **230** 2739